Deduction of the bond law from test on short RC tie in service conditions

Received: 28 November 2022 | Revised: 7 July 2023 | Accepted: 25 July 2023

DOI: 10.1002/suco.202201146

ARTICLE

fib CEB-FIP WILEY

Deduction of the bond law from test on short RC tie in service conditions

Pier Giorgio Debernardi | **Maurizio Taliano**

Department of Structural, Geotechnical and Building Engineering, Politecnico di Torino, Turin, Italy

Correspondence
Maurizio Taliano, Department of Structural, Geotechnical and Building Engineering, Politecnico di Torino, Turin, Italy.
Email: maurizio.taliano@polito.it

Abstract

Bond between ordinary steel bars and concrete plays a fundamental role in the behavior of the reinforced concrete. It is associated to the slip between steel and surrounding concrete and determines the variation in the steel and concrete stresses of cracked RC members. The need to formulate simple constitutive bond laws has led the international standards, such as *fib* Model Code 2010, to adopt an average bond stress versus slip relationship obtained from an extensive experimental campaign based on pull-out tests. However, in pull-out tests bond is substantially influenced by the state of stress, deformation and cracking of the concrete. Moreover, in-service conditions of RC members, in order to study the cracking behavior or the tension stiffening, an ascending distribution of the bond stress is usually considered as it corresponds to an ascending distribution of the slip from the zero slip section to the cracked section and in the literature the bond law is applied as it is. In particular, at the cracked section, the bond stress is maximum. But, this distribution of the bond stress is not confirmed by the experimental results available in the literature concerning the behavior of an RC tie with a length equal to the crack spacing, where close to the cracked sections a descending distribution of the bond stress is observed while the distribution of the slip remains ascending, with null bond stress at the cracked section. The modeling proposed here does not claim to be exhaustive due to the limited albeit accurate experimental data. However, it does indicate the opportunity to abandon bond laws based on experimental works that do not represent the real situation or are far from it.

KEYWORDS

bond law, bond stress, short RC tie, slip

1 | INTRODUCTION

Bond between ordinary steel bars and concrete plays a fundamental role in the behavior of the reinforced concrete. There is no reinforced concrete without a bond.

The first contribution to bond is given by the chemical and physical adhesions between steel and concrete.[1] This is followed by a mechanical interlocking between the bar ribs and the surrounding concrete. On the basis of the specific stress state, that is applied on an RC

member, the bond response is substantially modified. In effects, the same experimental methods, that are adopted to study the bond response, play a fundamental role leading to very different results. To this regard, in the pull-out test[2] shown in Figure 1a bond is determined from a tensile test on a steel bar embedded into a concrete prism for a length equal to 5 times the bar diameter, contrasting against a perforated steel plate placed at the base of the concrete prism. From the test, in addition to the applied force, the slip of the free end of the bar and the top face of the concrete prism is measured. In the pull-out test bond is favored by the concrete struts that form for the transmission of the forces from the plate to the embedded part of the steel bar and from the confinement exerted at the base of the concrete prism due to the friction between plate and concrete. A significant improvement in bond can be achieved with further transverse confinement, for example, with stirrups or transverse compression forces. Other versions of pull-out test can be found in the literature. For example, in the one proposed by Chapmann and Shah[3] (Figure 1b), two bars of different lengths, embedded into a concrete prismatic specimen, are put in tension and separated in order to eliminate any interaction of forces between them. In this case, the favorable effects mentioned above are not present and the bond stress is substantially different. The embedded bars were separated, rather than put end to end as in the Danish test,[4] to eliminate any interaction of forces between them.

A further typology of bond test is represented by the beam-test[5] (EN 10080, 2005), where two prismatic concrete blocks, reinforced by transverse stirrups, are interconnected at the bottom by a reinforcing bar, that is bonded at each block to the concrete on a length equal to 10 times the bar diameter, and at the top by a steel hinge (Figure 1c). The tension stress in the bar is introduced at the mid-span section of the test beam, by simple bending, applying on the test beam two equal forces disposed symmetrically with regard to the mid-span section. Concrete is, therefore, subjected to a biaxial state of stress that is made more complex by the confinement of the stirrups and the transmission mechanism of the bond forces.

In the above experimental test methods, bond is influenced by various mechanisms of transmission of forces that strongly modify the way the bond stresses are transferred.

In this paper, the experimental behavior in service conditions of an RC tie with a length equal to the crack spacing, named short RC tie, is considered. From this study, the experimental distribution of the bond stress along the tie axis is obtained and compared to the theoretical results available in the literature.[6–10] A theoretical formulation of the bond law is also proposed through two constitutive relationships with origins at the sections of zero slip and maximum slip.

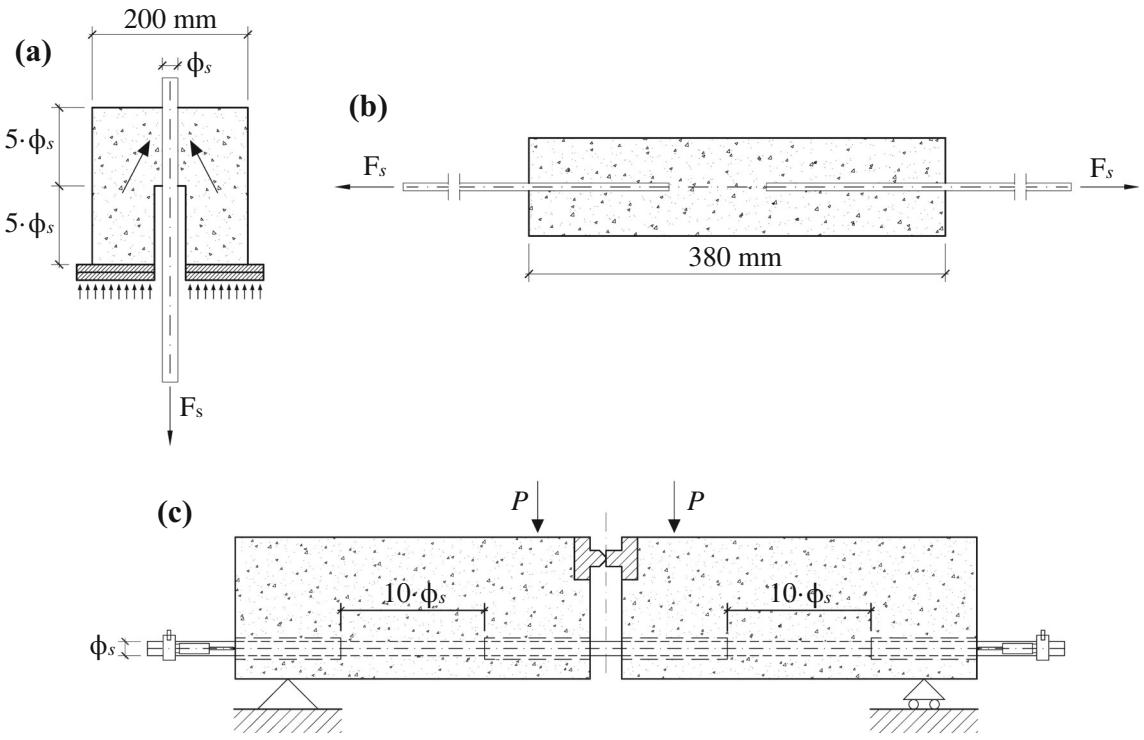

FIGURE 1 Pull-out testing methods according to: (a) RILEM/CEB/FIP[2]; (b) Chapman and Shah[3]; (c) EN 10080[5] (beam test).

2 | BOND MODELING IN INTERNATIONAL STANDARDS

The need to formulate simple constitutive laws has led the international standards to adopt an average bond stress versus slip relationship. To this regards, *fib* Model Code 2010,[11] in case of monotonic loading and pull-out failures, provided that splitting failures are avoided, proposes the so-called *fib* bond law (Figure 2). The parameters s_1, s_2, s_3, and τ_{max} that are shown in Figure 2 are defined on the basis of the bond condition assumed for the deformed bar. This relationship was obtained from an extensive experimental campaign based on pull-out tests.[12] However, in the literature its use is usually extended to RC members subjected to axial force, bending or bending and shear, without considering that the boundary conditions can be very different from the conditions that occur in a pull-out test. In particular, the first branch of the *fib* bond law, included between the slips $s_s = 0$ and $s_s = s_1$, that is represented by the following exponential equation (e.g., $s_1 = 1.0$ mm and $\alpha = 0.4$):

$$\tau_{bs} = \tau_{max} \cdot \left(\frac{s}{s_1}\right)^{\alpha} \quad 0 \le s \le s_1 \tag{1}$$

is often applied in-service conditions to study the tension-stiffening effect or for cracking analyses. In effects, under usual service conditions, the maximum values of slip vary from 0.1 to 0.2 mm for crack widths from 0.2 to 0.4 mm, well less than 1.0 mm. This first part is characterized by local crushing and micro-cracking and refers to the stage in which the ribs penetrate into the mortar matrix.[13]

Moreover, close to a transversal crack, Section 6.1.1.2 of *fib* Model Code 2010 proposes a linear reduction of the bond stress within a zone of constant length equal to twice the bar diameter. This zone of reduced bond is associated to a local phenomenon of disturbance due to the crack on the distribution of the bond stress.

In this context, in the following section, a simple case study in service conditions is examined showing that the application of the *fib* bond law, as it is, is clearly contradicted by the experimental results.

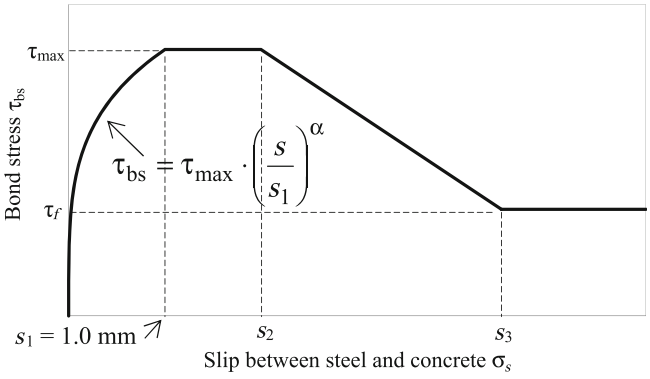

FIGURE 2 Bond law proposed by *fib* Model Code 2010.

3 | SHORT RC TIE REINFORCED BY A SINGLE BAR

3.1 | Theoretical analysis available in the literature

A short concrete tie of length L (Figure 3a), reinforced by a single deformed steel bar of diameter ϕ_s and transverse area A_s perfectly centred in the concrete section, is considered. It is assumed that at each free end of the bar an increasing axial force, F_s, in tension, is applied in service conditions and no further primary cracks occur along the short RC tie. At these sections, the steel stress, σ_{s2}, is maximum and equal to F_s/A_s, while the concrete stress is null. Conversely, at the mid-span section of the short RC tie, thanks to the bond between steel and concrete, the steel stress, σ_{sE}, is smaller than σ_{s2}, while the concrete stress σ_{cE} is greater than zero (Figure 3b). The maximum slip, $s_{s,max}$, occurs at the end faces of the short RC tie (Figure 3c), whereas the minimum slip is zero at the mid-span section owing to anti-symmetry conditions.

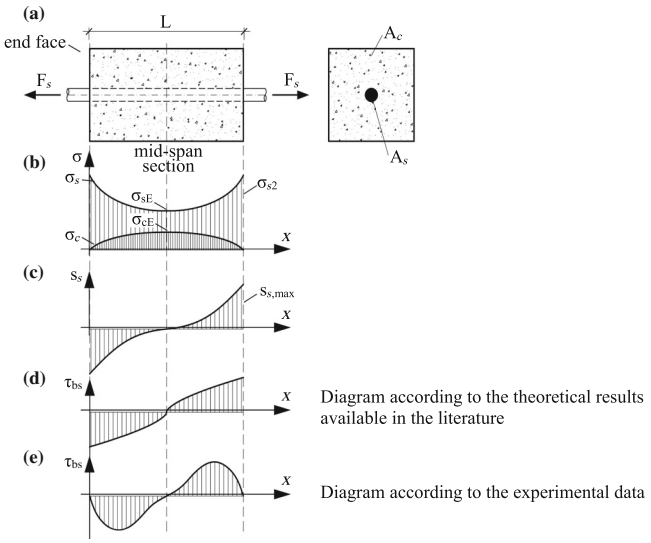

FIGURE 3 Comparison between the theoretical distributions of the bond stress obtained from cracking analyses available in the literature and the experimental distribution of the bond stress: (a) short RC tie; (b) theoretical steel and concrete stresses; (c) theoretical or experimental slip; (d) theoretical bond stress; (e) experimental bond stress.

If one associates, to each value of slip, the bond stress, τ_{bs}, that corresponds to the *fib* bond law as it is (Equation (1)), a monotonic distribution of the bond stress along the member axis can be obtained (Figure 3d). This monotonic distribution of the bond stress is consistent with many cracking analyses on RC tie available in the literature.[6–10] However, on the basis of the experimental results different conclusions can be drawn, anticipated in Figure 3e.

3.2 | Experimental analysis based on the distribution of the steel strain along the bar

3.2.1 | Premise

In the literature, some research works have provided the experimental distributions of the steel strain along the bar. The best results are those obtained by means of electrical strain gauges applied on the bar surface or inside the bar. To this regard, with reference to tensile tests on concrete ties reinforced by a central bar, Beeby and Scott[14] show a diagram of the steel strain ε_s over a length of 1200 mm for various load levels (Figure 4). In condition of stabilized cracking, outside the lateral zones where the external forces are introduced into the member, three peaks can be distinguished for the steel strain, indicating the position of as many primary cracks. And the steel strain reaches two minimum values between these three consecutive cracks. It is worth noting that, between each maximum and minimum values of the steel strain, an inflection point of the experimental curves can be observed. Since, to each steel strain, an elastic steel stress σ_s corresponds, the variation of σ_s along the axis is due, for the equilibrium condition, to a bond stress τ_{bs}, according to the following relationship:

$$\tau_{bs} = \frac{E_s \cdot \phi_s}{4} \cdot \frac{d\varepsilon_s}{dx}. \tag{2}$$

From Equation (2) it is evident that, where the steel strain is maximum or minimum, the first derivative $d\varepsilon_s/dx$ is null, and the bond stress is null as well. Moreover, at each inflection point of the steel strain (or the steel stress), the second derivative of steel strain is null. Therefore, according to Equation (2) each inflection point indicate the position where the bond stress shows a horizontal tangent or, that is the same, reaches a maximum (positive) or a minimum (negative) value.

These considerations are even more evident and clear in the Ujike's tests[15] (Figure 5) and in the Dey et al.'s tests[16] (Figure 6). Both tests are carried out on uncracked short RC prisms, where the strain gauges

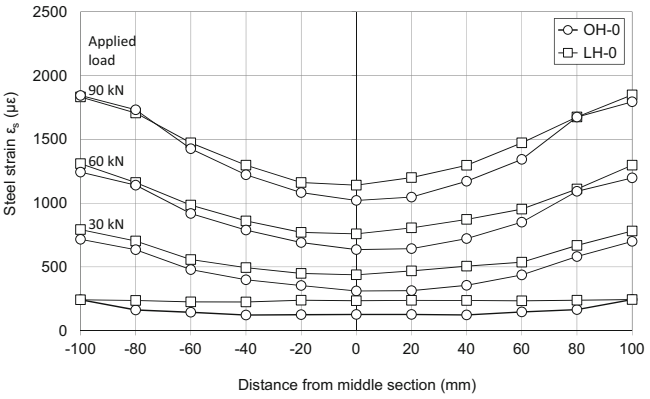

FIGURE 5 Experimental distributions of the steel stress at various levels of axial load from Ujike's tests.[15]

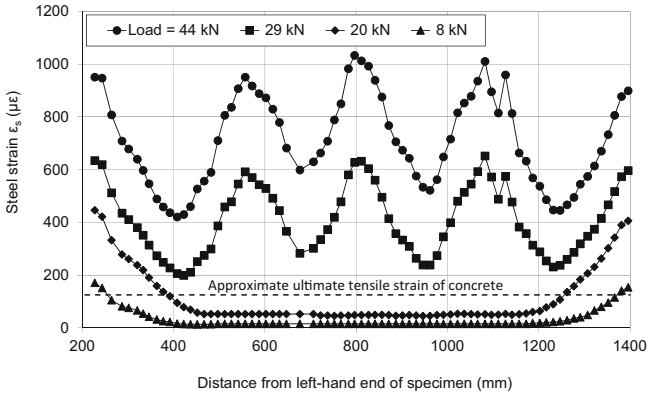

FIGURE 4 Experimental distributions of steel strain at various levels of axial load from the Beeby and Scott's test on specimen T16B1 (Beeby and Scott, 2005).

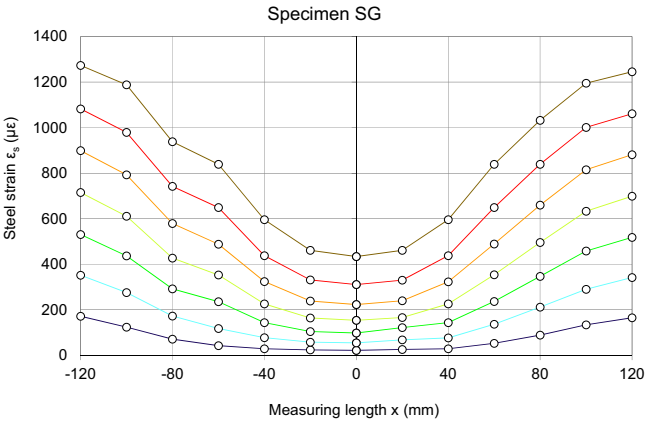

FIGURE 6 Experimental distributions of the steel strain between the two end faces of the short RC tie obtained in the Dey et al.'s test[16] at various levels of axial load.

were applied in some cases on the bar surface and in others inside the bar. In both experimental works, the distributions of the steel strain are obtained for different load levels. What is immediately evident is the different shapes that assume the experimental distribution of the steel strain along the bar axis (Figures 4–6) when compared to the theoretical one (Figure 3b). In effects, the experimental curves present two inflection points, located almost symmetrical with respect to the mid-span section, that are not present in the theoretical curve. This aspect is analyzed in detail below with reference to the experimental results obtained by Dey et al. (Figure 7) with the use of strain gauges applied inside the bar in such a way as not to interfere with the steel–concrete interface. This experimentation requires a rather delicate and long preparation, but it allows us to obtain more correct and detailed results.

3.2.2 | Analysis of the Dey et al.'s data

A tie with a length of 240 mm and cross-sectional area of concrete $A_c = 22{,}186\ \text{mm}^2$ is reinforced by a single instrumented bar 20-mm-diameter (Figure 7). The bar is instrumented making a longitudinal cut from two different 20 mm diameter steel bars, milling a small longitudinal groove 10 mm × 2 mm through the entire length of each half of the bar, placing 15 strain gauges inside the groove 20 mm apart and, finally, attaching the two halves of the bar with epoxy glue. The obtained bar has transverse area $A_s = 270.8\ \text{mm}^2$. The short RC tie is made of concrete with mean values of compressive strength $f_{cm} = 44.8$ MPa and elastic modulus $E_{cm} = 33.787$ GPa. The elastic modulus of steel, $E_s = 201.734$ GPa, is determined from uniaxial tests performed on 20-mm-diameter bars.

Assumed the symmetry of the short RC tie with respect to the mid-span section, the only right side of the distributions of the steel strain is considered, as on this side the distributions appear more regular than on the left side. Therefore, the part of the short RC tie considered for the analysis has a length of 120 mm. On it seven electrical strain gauges are arranged, with a pitch $p = 20$ mm. The strain gauges are identified by an index, i, that varies from 0 to 6, where $i = 0$ corresponds to the strain gauge placed at the mid-span section, $i = 6$ corresponds to that one at the end face of the short RC tie. An abscissa, x, is introduced along the bar axis with origin coincident with the mid-span section. So doing, the middle of each measurement location is identified by the abscissa x_i:

$$x_i = i \cdot p. \tag{3}$$

From the test the distributions of the steel stress, $\sigma_{s,i}$, are obtained (Figure 8), for various axial forces applied, multiplying the steel strains, $\varepsilon_{s,i}$, measured at seven locations along the axis of the bar, by the elastic modulus of steel.

The difference between the applied axial force and the resultant of the steel stresses gives the resultant of the concrete stresses, from which the distribution of the concrete stress along the bar is obtained (Figure 9).

From the difference of the steel stresses, $\sigma_{s,i+1}$ and $\sigma_{s,i}$, between two consecutive measurement locations, the bond stress, $\tau_{bs,i}$, can be determined:

$$\tau_{bs,i} = \frac{(\sigma_{s,i+1} - \sigma_{s,i}) \cdot A_s}{\pi \cdot \phi_s \cdot p}. \tag{4}$$

The bond stress, $\tau_{bs,i}$, represents the average value of bond stress referred to a length of 20 mm, between the abscissas x_i and x_{i+1}. Further values of the bond stress at the various measurement locations of abscissa x_i, are then determined by linear interpolation. The distributions of values of the bond stress are shown in Figure 10 as a function of the relevant abscissas, that means the abscissa of the middle points of each interval $[x_i; x_{i+1}]$ and the abscissa x_i, respectively, for various load levels.

By integrating the strains of steel and concrete along the bar axis, the elongations of steel and concrete with reference to the mid-span section, $u_{s,i}$ and $u_{c,i}$, at each measurement location, can be obtained:

$$u_{s,i} = \int_{x=0}^{x_i} \varepsilon_s \cdot dx, \tag{5}$$

$$u_{c,i} = \int_{x=0}^{x_i} \varepsilon_c \cdot dx. \tag{6}$$

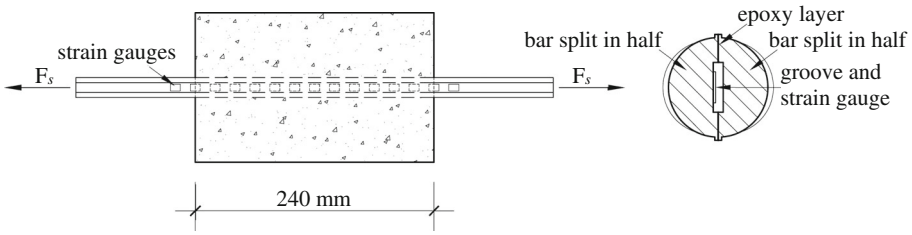

FIGURE 7 Strain gauge arrangements inside the RC short tie in the Dey et al.'s test.[16]

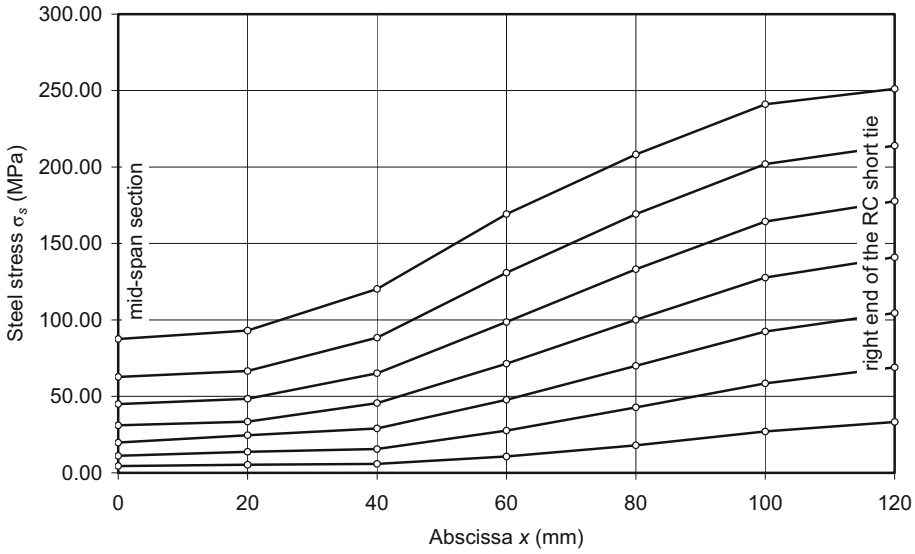

FIGURE 8 Experimental distributions of the steel stress, $\sigma_{s,i}$, as a function of the abscissa located between the mid-span section and the right end face of the short RC tie, obtained in the Dey et al.'s test[16] at various levels of axial load.

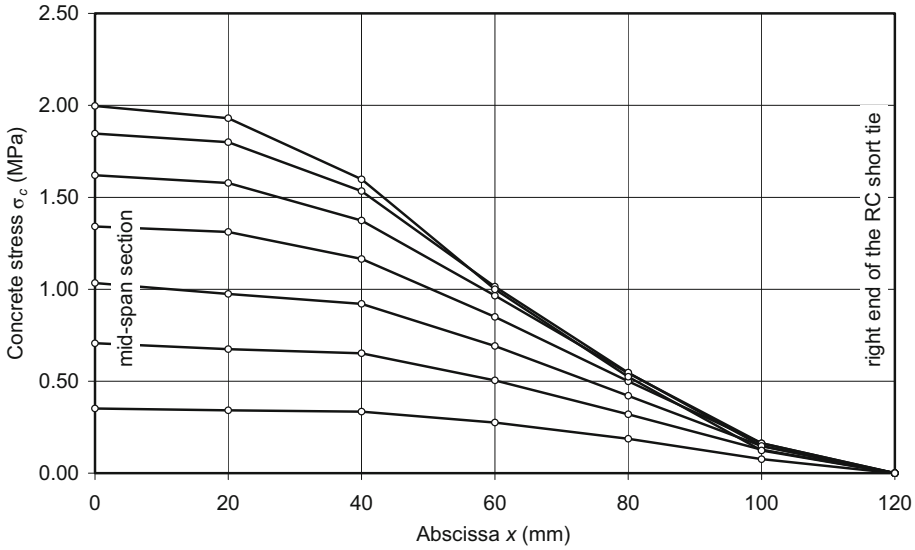

FIGURE 9 Experimental distributions of the mean concrete stress in the section, $\sigma_{c,i}$, as a function of the abscissa located between the mid-span section and the right end face of the short RC tie, obtained in the Dey et al.'s test[16] at various levels of axial load.

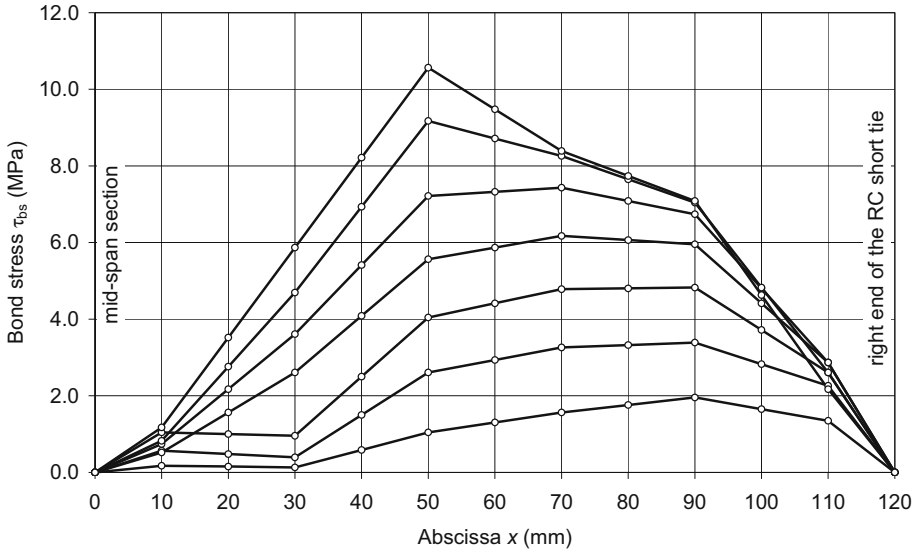

FIGURE 10 Experimental distributions of the bond stresses, $\tau_{bs,i}$, as a function of the abscissa located between the mid-span section and the right end face of the short RC tie, obtained in the Dey et al.'s test[16] at various levels of axial load.

Their difference provides the slip between steel and concrete at each measurement location:

$$s_{s,i} = u_{s,i} - u_{c,i}. \quad (7)$$

Figure 11 shows the distributions of the slip, $s_{s,i}$, along the member axis, for various load levels, as a function of the relevant abscissas.

Comparing Figures 10 and 11 it appears that the distributions of the slip are increasing along the whole bar axis reaching a maximum value at the end face of the short RC tie, while the distributions of the bond stress reach a maximum value somewhere along the bar axis becoming null at its end face. In other words, near the mid-span section both the values of the bond stress and the slip are increasing, but near the end face of the short RC tie the bond stress decreases even though the slip is increasing. As an example to better clarify this observation, Figure 3e shows a schematic representation of the experimental results to which this papers refers. This is clearly in contrast with what is obtained in the literature[6–10] (Figure 3d).

Some authors consider this effect as a damage of bond in reinforced concrete produced by secondary and Goto cracks,[17] limited to the zone adjacent to the crack.[14,16] But, observing carefully the experimental distributions of the bond stress along the bar axis (Figure 10), this phenomenon already occurs for small levels of axial force and the length of the affected zone increases as the axial force increases till it extend to most of the zone between the mid-span section and the end face of the short RC tie. A theoretical model that considers a zone of reduced bond with a length that increases with the applied force was already proposed by the same authors,[18,19] obtaining interest in the literature.[20]

It is worth noting that the distribution of the bond stress along the tie axis is deduced directly from the experimental distribution of the steel strain. In the sense that it does not depend on the assumption adopted for the distribution of the concrete stresses on the section.

Finally, by associating the values of the slip to the relevant values of the bond stress, the curves of the bond stress versus slip, $\tau_{bs,i}$–$s_{s,i}$, can be obtained for various levels of axial load (Figure 12). These curves are formed by two distinct branches. The first branch shows increasing values of the bond stress and is followed by a second descending branch. These results are astonishing and unexpected if one reasons with the *fib* bond law as it is. In effects, according to the modeling of the *fib* Model Code 2010[11] (Equation (1)), up to a slip $s_s = s_1 = 1$ mm, the values of the bond stress are always increasing along the whole transmission length as the values of the slip are increasing. Evidently, the experimental results require a rethinking of the correct use of the bond law in service conditions for the determination of the tension-stiffening effect and the crack opening. Moreover, what happens is not just a local phenomenon, but has to be considered as preponderant in-service conditions in case of stresses close to the maximum values.

4 | SIMPLIFIED BOND LAW

It is certainly not from the results of very few tests that such a complex modeling of the experimental behavior can be defined. However, on the basis of the good quality

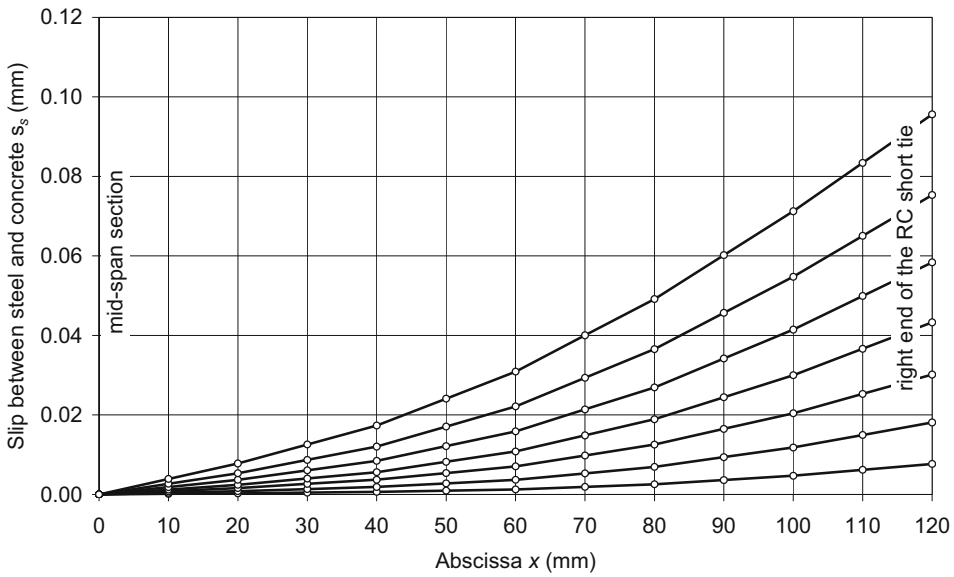

FIGURE 11 Experimental distributions of the slip, $s_{s,i}$, as a function of the abscissa located between the mid-span section and the right end face of the short RC tie, obtained in the Dey et al.'s test[16] at various levels of axial load.

of the experimental results, it is possible to identify a tendency of the behavior.

From the examination of the bond stress–slip diagrams (Figure 12), starting from the mid-span section, a first ascending branch is observed which, as a first approximation, can be considered linear for the various load levels:

$$\tau_{bs} = k_1 \cdot s_s \tag{8}$$

and, in the present case, it can be assumed that $k_1 = 465$ N/mm^3 independently on the applied load level.

A more refined equation could be proposed on the basis of further tests. Equation (8) can be applied in the zone of the transmission length near the mid-span section, for a distance L_1, that is a priori unknown.

The descending branch is observed in Figure 12 near the end face of the short RC tie, where internal cracks occur as demonstrated by Goto.[17] It cannot be obtained from pull-out tests as in this type of bond test the local behavior is governed by the presence of concrete struts. The type of bond test that could be representative of the descending branch is that one proposed by Chapmann and Shah.[3] In effects, at the end face of the short RC tie, a null bond stress corresponds to the maximum slip, s_{max}. For a slip $s_s < s_{max}$, in the zone influenced by secondary and Goto cracks of length L_{sc}, it can be assumed, albeit with less precision, the following distribution of the bond law:

$$\tau_{bs} = k_2 \cdot (s_{s,max} - s_s)^{0.5}, \tag{9}$$

where, in the present case, it can be assumed that $k_2 = 40$ N/mm$^{5/2}$ independently on the applied load level. Also in this case a refined equation could be adopted on the basis of consolidated data.

The bond laws corresponding to Equations (8) and (9) for various load levels are represented in Figure 13 and compared to the bond stress versus slip relationships obtained experimentally.

5 | SIMPLIFIED CALCULATION PROCEDURE

A simplified evaluation of the bond stresses along the steel-concrete interface in a short RC tie subjected to a monotonic tensile force, F_s, is here proposed.

Given the force F_s, the steel stress at the end face of the short RC tie, $\sigma_{s2} = F_s/A_s$, is determined, while the steel stress at the zero slip section, σ_{sE}, is unknown and depends on the distribution of the bond stress, τ_{bs}. Therefore, it is necessary to refer to the two bond laws expressed by Equations (8) and (9) to be applied along the zones close to the zero slip section and the end face of the short RC tie, respectively.

Although other functions are possible, the distribution of the slip can be represented by a parabola of equation:

$$s_s = A \cdot x^2 + B \cdot x \text{ For } \quad 0 \le x \le L/2. \tag{10}$$

Assuming tentative values for the coefficients A and B, starting from the mid-span section ($x = 0$), the ascending bond law, Equation (8), is adopted, while starting from the end face of the short tie ($x = L/2$) the descending bond law, Equation (9), is used till the intersection with the ascending bond law. Therefore, a tentative distribution of the bond stress can be obtained between the zero slip section and the end face of the

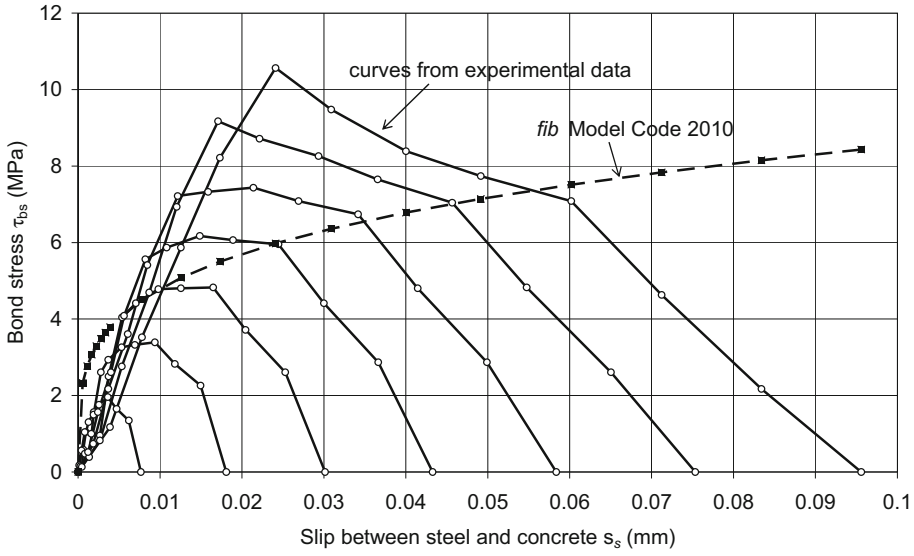

FIGURE 12 Experimental diagrams of the bond stress versus slip, $\tau_{bs,i}$–$s_{s,i}$, at various levels of axial load obtained in Dey et al.'s test[16] along the right side of the short RC tie and the *fib* bond law (obtained with: $f_{cm} = 44.8$ MPa; $f_{ck} = f_{cm} - 8 = 36.8$ MPa; $\alpha = 0.25$).

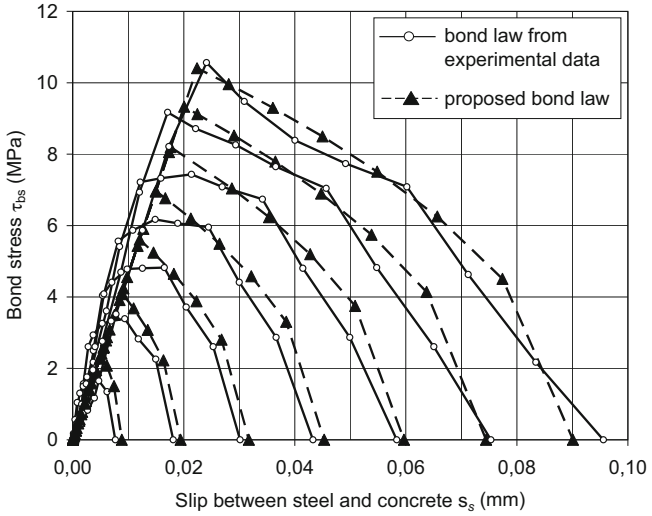

FIGURE 13 Comparison between the experimental diagrams of the bond stress versus slip, τ–s_s, (continuous lines with white circular boxes) obtained by Dey et al.[16] on the right side of the short RC tie at various levels of axial load and the theoretical results of the proposed simplified model (dotted lines with black triangular boxes).

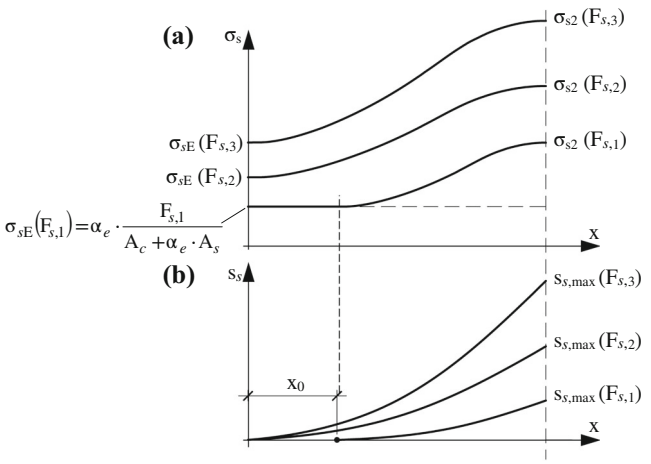

FIGURE 14 Schematic distributions of the steel stress (a) and the slip (b) between the mid-span section and the right end face of the short RC tie at various levels of axial load ($F_{s,1} < F_{s,2} < F_{s,3}$).

short RC tie, to which the following resultant of the bond forces corresponds:

$$R_\tau = \pi \cdot \phi_s \cdot \int_0^{L/2} \tau_{bs} \cdot dx. \tag{11}$$

At the zero slip section the resulting force applied to the steel bar is equal to the difference of the forces F_s–R_τ, while the steel and concrete stresses result:

$$\sigma_{sE} = \frac{F_s - R_\tau}{A_s}, \tag{12}$$

$$\sigma_{cE} = \frac{R_\tau}{A_c}. \tag{13}$$

New distributions of the steel and concrete elongations, u_s and u_c, and the slip s_s can be determined accordingly.

The mathematical problem presents two unknowns, which means the A and B coefficients of Equation (10). These coefficients A *e* B can be replaced by the tentative values of slip at the cracked section, $s_{x=L/2}$, and at the half of the considered interval, $s_{x=L/4}$, through the following equations:

$$A = \frac{s_{x=L/2} - B \cdot L/2}{(L/2)^2}, \tag{14}$$

$$B = -\frac{s_{x=L/2} - 4 \cdot s_{x=L/4}}{L/2}. \tag{15}$$

An iterative procedure is, therefore, performed which gives at each iteration new values of slip $s^{IT}_{x=L/4}$ and $s^{IT}_{x=L/2}$, calculated as a function of the distributions of the steel and concrete strains, to be compared to those assumed in the previous iteration.

For low levels of the axial force, F_s, the distribution of the slip may not affect the entire length between the mid-span section ($x = 0$) and the cracked section ($x = L/2$). This means that at the mid-span section, the steel is perfectly bonded to the concrete (the slip is null), the condition of plane section occurs and the steel and concrete stresses are known (curve $F_{s,1}$ of Figure 14). The zero slip section does not coincide with the mid-span section but is located at the abscissa $x = x_0$.

From the zero slip section ($x = x_0$) and the cracked section ($x = L/2$) the distribution of the slip can still be assumed with a parabolic law:

$$s_s = A \cdot (x - x_0)^2 \quad \text{for} \quad x_0 \le x \le L/2. \tag{16}$$

The B coefficient is put equal to zero as required by the condition of perfect bond ($\varepsilon_s = \varepsilon_c$) at the zero slip section.

The problem still presents two unknowns, which means the length x_0 and the A coefficient. An iterative procedure is needed also in this case to fulfill the equilibrium and congruency conditions.

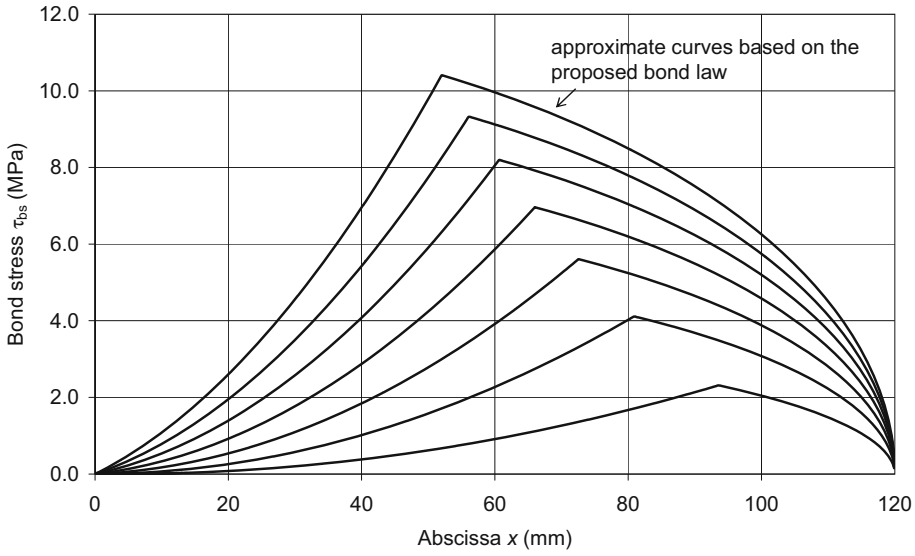

FIGURE 15 Theoretical distributions of the bond stress obtained according to the proposed simplified model along the right side of the short RC tie at various levels of axial load (Dey et al.'s test[16]).

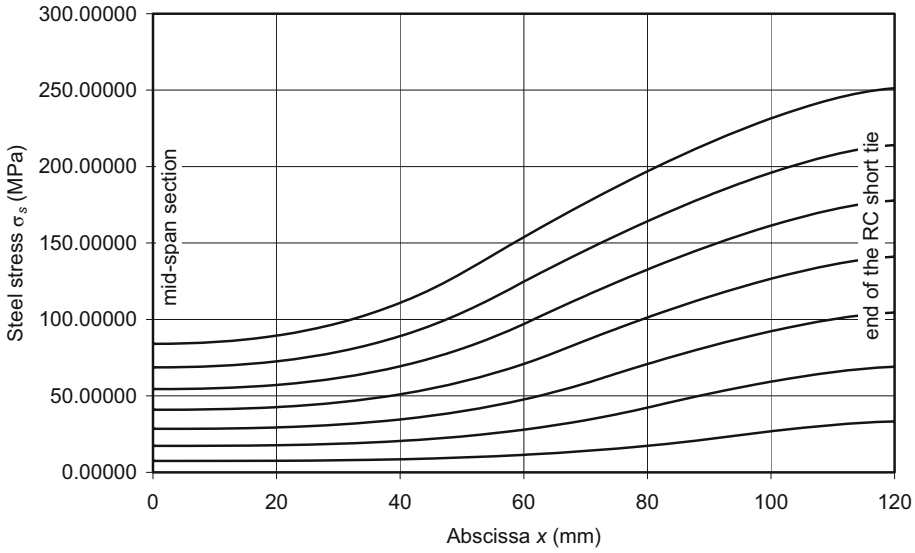

FIGURE 16 Theoretical distributions of the steel stress obtained according to the proposed simplified model along the right side of the short RC tie at various levels of axial load (Dey et al.'s test[16]).

As an example of application, Dey et al.'s test[16] is considered when the applied force F_s varies from 9.0 to 68.0 kN. In Figures 15 and 16 the theoretical distributions of the bond stress and the steel stress are shown as a function of the abscissa of the short RC tie, respectively.

For a comparison with the experimental results, it would be also necessary to take into account the effect of the shrinkage.

6 | CONCLUSIONS

In service conditions, when a bond needs to be taken into account, such as for the analysis of the tension stiffening and the cracking behavior, it is often considered sufficient to assume a uniform distribution of an average bond stress along the interface between steel and concrete. The bond law proposed by international standards is used in the most important cases or in research, even though, as far as the *fib* bond law, limited to the first branch only, since the values of the slip are less than 1.0 mm. In these situations, if one applies the *fib* bond law as it is, an ascending distribution of the bond stress corresponds to an ascending distribution of the slip from the zero slip section to the cracked section. However, this is not confirmed by the experimental results available in the literature concerning the behavior of a short RC tie, where close to the cracked sections descending distributions of the bond stress are associated to ascending distributions of slip. Some authors consider this effect as a damage of bond in reinforced concrete produced by secondary and Goto cracks, limited to the zone adjacent to the crack. But, the experimental evidence shows that this phenomenon already occurs for small levels of axial force

and the length of the affected zone increases as the axial force increases till it extend to most of the zone between the mid-span section and the end face of the short RC tie. The corresponding bond stress–slip diagram, obtained from the experimental data, clearly shows two distinct branches: a first approximately linear branch in which, starting from the zero slip section, the bond stress and the slip both increase; a second branch in which the bond stress decreases when the slip continues to increase. Therefore, what happens is not just a local phenomenon, but has to be considered as preponderant in-service conditions in case of stresses close to the maximum values.

The modeling proposed here, although simplified from a conceptual point of view, does not claim to be exhaustive due to the limited albeit accurate experimental data. However, it does indicate the opportunity to abandon bond laws based on experimental works that do not represent the real situation or are far from it. Therefore, these bond laws are not adequate to study the cracking behavior of RC members subjected to axial force or bending. On the contrary, when a cracking analysis is performed it is necessary to adopt two bond laws along the transmission length in order to respect the basic assumptions (e.g., no further cracks can form in case of stabilized cracking, maximum crack spacing equal to twice the transmission length) and the equilibrium and congruency conditions. Both two bond laws are applied from sections where the bond stress is null: the first at the zero slip section, the second at the end face of the short RC tie where the slip is maximum. Their validity remain till their intersection.

In this regard, in previous works the authors already introduced the need to consider two different bond laws in the transmission length for cracking problems, but this arised some criticism from researchers. The authors believe that the experimental results found may dispel further doubts.

CONFLICT OF INTEREST STATEMENT

The authors declare no conflicts of interest.

DATA AVAILABILITY STATEMENT

Data sharing not applicable to this article as no datasets were generated or analysed during the current study.

ORCID

Maurizio Taliano https://orcid.org/0000-0002-5217-6222

REFERENCES

1. Eligehausen R, Bigaj-van VA. 3.3.2 Bond behaviour and models *fib* Bulletin N. 51. Structural concrete—Textbook on behaviour, design and performance—Volume 1. Lausanne: International Federation for Structural Concrete (fib); 2009.
2. RILEM/CEB/FIP. Test and specifications of reinforcements for reinforced and prestressed concrete. Four recommendations of the RILEM/CEB/FIP Committeee 2: pull-out test. Materials and Structures, RILEM. 1970;3(15):147–78.
3. Chapman RA, Shah SP. Early-age bond strength in reinforced concrete. ACI Materials Journal. 1987;84(6):501–10.
4. Danish Standards Organization. DS 2082 - pullout test, Copenhagen. 1980 2 pp.
5. CEN. EN 10080—steel for the reinforcement of concrete—weldable reinforcing steel—general, European Committee for Standardization. 2005.
6. Tue N, Konig G. Calculating the mean bond and steel stress in reinforced and prestressed concrete members. Darmstadt Concrete. 1991;6:77–86.
7. Balázs GL. Cracking analysis based on slip and bond stresses. ACI Materials Journal. 1993;90(4):340–8.
8. Balázs GL. 4.3.2 crack control, fib bulletin N. 52. Structural concrete—textbook on behaviour, design and performance—Volume 2. Lausanne: International Federation for Structural Concrete (fib); 2009.
9. Tan R, Eileraas K, Opkvitne O, Žirgulis G, Hendriks MAN, Geiker M, et al. Experimental and theoretical investigation of crack width calculation methods for RC ties. Structural Concrete. 2018;19:1436–47.
10. Schlicke D, Dorfmann EM, Fehling E, Tue NV. Calculation of maximum crack width for practical design of reinforced concrete. Civil Engineering Design. 2021;3:45–61.
11. Fédération Internationale du Béton (fib). *fib* Model Code for Concrete Structures 2010. Berlin, Germany: Ernst & Sohn; 2013.
12. Eligehausen R, Popov EP, Bertero VV. Local bond stress—slip relationships of deformed bars under generalized excitations: experimental results and analytical model. Report No. UCB/EERC 83/23, Berkeley, University of California 1983.
13. Balázs GL, Jaccoud JP, et al. Serviceability models—behaviour and modelling in serviceability limit states including repeated and sustained loads. CEB Bulletin N. 235, Lausanne 1997.
14. Beeby AW, Scott RH. Cracking and deformation of axially reinforced members subjected to pure tension. Magazine of Concrete Research. 2005;57(10):611–21.
15. Ujike I. Experimental study for effect of concrete shrinkage on behaviour of bond in reinforced concrete member. Bond in concrete—from research to standards, proceedings. Budapest: Budapest University of Technology and Economics; 2002. p. 238–45.
16. Dey A, Bado MF, Sokolov A, Kaklauskas G. Distributed sensing, fiber Bragg gratings and strain gauges for strain monitoring of RC tensile element. Fib Symposium 2020, concrete structures for resilient society 22–24 November, 2020. China: Shanghai; 2020.
17. Goto Y. Cracks formed in concrete around deformed tension bars. ACI Journal. 1971;68(4):244–51.
18. Debernardi PG, Guiglia M, Taliano M. Effect of secondary cracks for cracking analysis of reinforced concrete tie. ACI Materials Journal. 2013;110(2):209–16.
19. Debernardi PG, Taliano M. An improvement to Eurocode 2 and *fib* model code 2010 methods for calculating crack width

in RC structures. Structural Concrete. 2016;17(3):365–76. https://doi.org/10.1002/suco.201500033
20. Barre F, Bisch P, Chauvel D, Cortade J, Coste J-F, Dubois J-P, et al. Control of cracking in reinforced concrete structures: research project CEOS.fr. London: Wiley-ISTE; 2016. p. 257.

AUTHOR BIOGRAPHIES

Pier Giorgio Debernardi, Department of Structural, Geotechnical and Building Engineering, Politecnico di Torino, Italy. Email: piergiorgio.debernardi@formerfaculty.polito.it.

Maurizio Taliano, Department of Structural, Geotechnical and Building Engineering, Politecnico di Torino, Italy. Email: maurizio.taliano@polito.it.

How to cite this article: Debernardi PG, Taliano M. Deduction of the bond law from test on short RC tie in service conditions. Structural Concrete. 2023;24(6):7009–20. https://doi.org/10.1002/suco.202201146